Environ. Sci. Technol. **2003**, *37,* 5701−5710

Fluorescence Excitation−Emission Matrix Regional Integration to Quantify Spectra for Dissolved Organic Matter

WEN CHEN,[†] PAUL WESTERHOFF,*[,‡] JERRY A. LEENHEER,[§] AND KARL BOOKSH[||]

Department of Civil and Environmental Engineering, Arizona State University, Box 5306, Tempe, Arizona 85287-5306, U.S. Geological Survey, Box 25046, MS 408, Denver Federal Center, Denver, Colorado 80225, and Department of Chemistry & Biochemistry, Arizona State University, Tempe, Arizona 85287

Excitation−emission matrix (EEM) fluorescence spectroscopy has been widely used to characterize dissolved organic matter (DOM) in water and soil. However, interpreting the >10,000 wavelength-dependent fluorescence intensity data points represented in EEMs has posed a significant challenge. Fluorescence regional integration, a quantitative technique that integrates the volume beneath an EEM, was developed to analyze EEMs. EEMs were delineated into five excitation−emission regions based on fluorescence of model compounds, DOM fractions, and marine waters or freshwaters. Volumetric integration under the EEM within each region, normalized to the projected excitation−emission area within that region and dissolved organic carbon concentration, resulted in a normalized region-specific EEM volume ($\Phi_{i,n}$). Solid-state carbon nuclear magnetic resonance (^{13}C NMR), Fourier transform infrared (FTIR) analysis, ultraviolet−visible absorption spectra, and EEMs were obtained for standard Suwannee River fulvic acid and 15 hydrophobic or hydrophilic acid, neutral, and base DOM fractions plus nonfractionated DOM from wastewater effluents and rivers in the southwestern United States. DOM fractions fluoresced in one or more EEM regions. The highest cumulative EEM volume ($\Phi_{T,n} = \Sigma\Phi_{i,n}$) was observed for hydrophobic neutral DOM fractions, followed by lower $\Phi_{T,n}$ values for hydrophobic acid, base, and hydrophilic acid DOM fractions, respectively. An extracted wastewater biomass DOM sample contained aromatic protein- and humic-like material and was characteristic of bacterial-soluble microbial products. Aromatic carbon and the presence of specific aromatic compounds (as indicated by solid-state ^{13}C NMR and FTIR data) resulted in EEMs that aided in differentiating wastewater effluent DOM from drinking water DOM.

Introduction

Dissolved organic matter (DOM) is a heterogeneous mixture of aromatic and aliphatic organic compound containing oxygen, nitrogen, and sulfur functional groups (e.g., carboxyl, phenol, enol, alcohol, carbonyl, amine, and thiol). DOM affects biogeochemical processes, particle stability and transport, metal complexation, and production of disinfection byproducts (DBPs) during water and wastewater treatment (*1*−*3*). Molecular weight distributions and UV absorption spectra have been used to characterize nonfractionated DOM; DOM is quantified as dissolved organic carbon (DOC) (*4*−*7*). More advanced characterization techniques such as carbon nuclear magnetic resonance (^{13}C NMR) spectroscopy or Fourier transform infrared (FTIR) spectroscopy require intensive sample preparation (i.e., DOM extraction/isolation and desalting) but permit quantification of specific classes of DOM compounds (*3*, *8*, *9*). In this paper, fluorescence spectroscopy of DOM, which requires minimal sample pretreatment, is applied to fractionated and nonfractionated DOM and uses a new analytical approach termed fluorescence regional integration (FRI).

Various fluorescence spectroscopy techniques have been used to characterize sources of marine, aquatic, and soil DOM samples (*9*−*11*). These include the following fluorescence techniques: (i) emission scan at fixed excitation wavelengths, (ii) synchronous scan at a constant offset wavelength (18, 20, 40, or 60 nm) between excitation (λ_{ex}) and emission (λ_{em}) wavelengths, and (iii) excitation−emission matrix (EEM) analysis (*12*−*16*). Although obtaining fluorescence data is relatively straightforward, techniques that quantify the properties of fluorescence spectra have been limited, usually using only one, two, or three data points from fluorescence spectra. Several fluorescence analysis techniques using a limited number of data points will be briefly reviewed. First, the fluorescence index (the ratio of emission intensity at 450 nm over 500 nm at 370 nm excitation) was used to distinguish microbially derived DOC sources from terrestrially derived sources (*17*−*19*). Second, synchronous fluorescence spectroscopy was used to differentiate natural organic matter (NOM) from wastewater-derived DOM and to detect the presence of these substances in the river water downstream of wastewater treatment plant (WWTP) discharges (*20*). Third, the rising slope of a fluorescence spectral peak and integration under the major peak emission spectra were used to determine concentrations of NOM fractions in nonfractionated water samples (*21*−*23*). Fourth, ratios of fluorescence EEM peak intensities were used to track changes in NOM in natural water systems (*24*). Fifth, on-line fluorescence intensity at 340 nm was related to 5-day biological oxygen demand in WWTPs (*11*).

Because existing techniques to quantify fluorescence spectra use only one to three data points from a spectrum that may contain 50 to >10,000 wavelength-dependent fluorescence intensity data points, the techniques just described lack the ability to capture the heterogeneity of aromatic DOM. Advances in fluorescence instrumentation can facilitate the handling of data from fluorescence scans and have popularized creation of EEMs. However, tools to quantitatively analyze EEM are lacking.

This paper introduces a quantitative method for analyzing fluorescence EEMs—the FRI technique. Spectral analysis—fluorescence, ultraviolet−visible (UV−Vis) absorption, solid-state ^{13}C NMR spectroscopy, and FTIR spectroscopy—was used to characterize DOM fractions (acids, bases, neutrals) and, along with model organic compounds, to delineate EEMs

* Corresponding author phone: (480)965-2885; fax: (480)965-0557; e-mail: p.westerhoff@asu.edu.

[†] PBS4J INC. 7310 N. 16th St. Ste 310, Phoenix, AZ 85020.

[‡] Department of Civil and Environmental Engineering, Arizona State University.

[§] U.S. Geological Survey.

[||] Department of Chemistry & Biochemistry, Arizona State University.

10.1021/es034354c CCC: $25.00
Published on Web 11/15/2003

TABLE 1. Description of DOM Sources Used for EEM Analysis

source	sample ID no.	DOC (mg/L)	$SUVA_{254}$ [m^{-1} $(mg/L)^{-1}$]	description
91st Ave. WWTP effluent				Nitrification/denitrification with chlorination
(Phoenix, AZ)	EHPO-N	1.0	1.63	hydrophobic neutral
	EHPO-A	1.0	1.52	hydrophobic acid
	E-Base	1.0	2.25	base
	EHPI-A	1.0	1.46	hydrophilic acid
	EHPI-N	1.0	0.67	hydrophilic neutral
91st Ave. WWTP pilot wetland				Pilot wetland system that receives 100% WWTP effluent
effluent (Phoenix, AZ)	EEHPO-N	1.0	1.50	hydrophobic neutral
	EEHPO-A	1.0	1.61	hydrophobic acid
	EE-Base	1.0	2.28	base
	EEHPI-A	1.0	1.46	hydrophilic acid
Salt River (Phoenix, AZ)				Stream not affected by upstream wastewater
	SHPO-A	1.0	1.90	hydrophobic acid
	S-Base	1.0	2.70	base
	SHPI-A	1.0	1.90	hydrophilic acid
Gila River (Phoenix, AZ)				Stream not affected by upstream wastewater
	GHPO-A	1.0	3.5	hydrophobic acid
Suwannee River (Georgia)	SRFA	1.0	4.2	Standard fulvic acid from IHSS
Biomass from WWTP (Mesa, AZ)	EBOM	1.0	1.50A	Alkaline-extractable DOM from activated sludge biomass
Drinking water				Nonfractionated DOM
Tucson, AZ	T-DW	0.20	3.65	unchlorinated groundwater
Mesa, AZ	M-DW	2.72	1.07	conventionally treated surface water
Wastewater				Nonfractionated DOM
Tucson, AZ	T-WW	18.0	1.45	trickling filter effluent
Mesa, AZ	M-WW	6.25	1.44	biologically denitrified effluent

into five regions. Quantitative analysis for the FRI technique included integration of the volume beneath each EEM region. A secondary objective was to contrast the spectral analyses of organic matter from surface water sources affected by wastewater and from those unaffected by wastewater. For example, the FRI technique was applied to DOM fractions and nonfractionated river and wastewater effluent samples. The FRI technique is among the first approaches to analyze DOM through quantitative use of all the wavelength-dependent fluorescence intensity data from EEMs.

Materials and Methods

EEM spectra were obtained for DOM fractions and nonfractionated water samples. Sample identification names for DOM fractions are defined in Table 1. Standard Suwannee River fulvic acid (SRFA), obtained from the International Humic Substance Society (IHSS), was used to validate the reproducibility of FRI as compared with other approaches to quantifying fluorescence and served as a readily available DOM source for comparison by other research groups. DOM fractions—including hydrophobic acids (HPO-A), neutrals (HPO-N), bases (Base), hydrophilic acids (HPI-A), and neutrals (HPI-N)—were fractionated, isolated, and concentrated by the U.S. Geological Survey (*8*, *25*) from three sites in metropolitan Phoenix, AZ: the Salt River, the Gila River, and the 91st Avenue WWTP effluent-treatment wetland (inlet to and outlet from the treatment wetland). The Salt River sample (18.4 L) was collected at Ballard Avenue on June 20, 1996. The Gila River sample (60 L) was collected just above its confluence with the Salt River in April 1997, and the 91st Avenue WWTP samples (40 L) were collected before and after the discharged effluent passed through a treatment wetland.

An extracellular biological organic matter (EBOM) fraction was extracted from activated sludge collected at the Northwest Wastewater Reclamation Plant (Mesa, AZ). The extraction involved 100 g of filtered (ashed Whatman glass fiber/coarse [GF/C] filter, Whatman, West Chester, PA) activated sludge biomass, to which 200 mL of ammonium hydroxide was added, slowly stirred for 30 min, and filtered (GF/C). The filtrate was cation-exchanged and lyophilized. Finished drinking water samples from Mesa, AZ (collected April 25, 2000), and Tucson, AZ (collected March 29, 2000), were collected along with samples from WWTPs in the same municipalities. Model organic compounds (e.g., tryptophan and tyrosine) were also analyzed.

All isolates were dissolved in Super-Q water (Millipore, Bedford, MA) containing 0.01 M KCl. All samples were filtered (ashed Whatman 0.7 μm GF/F, Whatman, West Chester, PA) and acidified with HCl to pH ~3. No precipitates were observed with the sample at pH 3.

Fluorescence EEM measurements were conducted using a Perkin-Elmer LS-50B luminescence spectrometer. The spectrometer displayed a maximum emission intensity of 1000 arbitrary units (AU). The spectrometer used a xenon excitation source, and excitation and emission slits were set to a 10-nm band-pass. To obtain fluorescence EEMs, excitation wavelengths were incrementally increased from 200 to 400 nm at 5-nm steps; for each excitation wavelength, the emission at longer wavelengths was detected at 0.5-nm steps. To limit second-order Raleigh scattering, a 290-nm cutoff was used for all samples. Quinine sulfate (QS) solution (1 μg of QS/L in 0.1 M H_2SO_4) was used to monitor the stability of energy emitted by the xenon lamp in the fluorometer (*26*), and no change in QS fluorescence was observed during the study. All samples were diluted to a final DOC of 1 mg/L with 0.01 M KCl or less than 1 mg/L if the sample had maximum fluorescence emission intensities exceeding 1000 AU (*27*). Emission spectra for all DOM fractions were collected at pH 3 and pH 8, but only minor differences were observed. However, to minimize the potential for metal-binding and subsequent fluorescence quenching in nonfractionated water sources that contains metals, only pH 3 data are presented.

To partially account for Raleigh scattering, the fluorometer's response to a blank solution was subtracted from the fluorescence spectra recorded for samples containing DOC. The blank solution was prepared from Super-Q water and contained <0.2 mg/L DOC. To account for absorbance of light from the lamp by DOC molecules, an inner-filter correction was applied to these data using UV—Vis spectra data (*27*, *28*). Samples were not corrected for the excitation response of the lamp source. Because all data were collected on a single instrument, the results were internally compa-

rable. The corrected EEMs were plotted using SigmaPlot 2001 (SPSS Inc.) with 20 contour lines; each contour interval represented 1/20th of the maximum fluorescence intensity.

DOC was measured using a Shimadzu TOC-5050A total organic carbon analyzer, which uses a medium-temperature catalytic oxidation method (Standard Method 5310B) (*29*). UV light absorption at 254 nm (UVA_{254}) and UV−Vis spectra were measured using a Shimadzu UV-1601 variable-wavelength spectrophotometer and a quartz cuvette with a 1-cm path length.

Infrared spectra were collected using 2−5 mg of NOM fraction isolates in KBr pellets. The Perkin-Elmer System 2000 FTIR used a glow bar source and a deuterated triglycine sulfate detector. The instrument was set up to scan from 4000 to 400 cm^{-1} averaging 10 scans at 1.0-cm^{-1} intervals with a resolution of 4.0 cm^{-1}. All spectra were normalized after acquisition to a maximum emission of 1.0 for comparative purposes.

Solid-state cross polarization magic angle spinning (CP-MAS) ^{13}C NMR spectra were obtained on 20−200 mg of NOM samples. Freeze-dried samples were packed in zirconia rotors. CPMAS ^{13}C NMR spectra were obtained on a 200-MHz Chemagnetics CMX spectrometer with a 7.5-mm-diameter probe. The spinning rate was 5000 Hz. The acquisition parameters included a contact time of 5 ms for the 91st Avenue WWTP effluent samples, a 1-ms contact time for the Salt and Gila River samples, a pulse delay of 1 s, and a pulse width of 4.5 μs for the 90° pulse. Studies of variable contact time indicate that a 5-ms contact time is optimum for quantitatively determining the contributions of different carbon structural groups to the DOM NMR spectra (*9, 30*). The Gila and Salt River samples were run with a 1-ms contact time because small sample size necessitated the greater signal sensitivity obtained at 1 ms.

Results and Discussion

Compound-Class Composition of DOM Fractions. The ^{13}C NMR and FTIR spectra of the DOM fractions of wastewater effluent from the 91st Avenue WWTP are presented in Figure 1, and the DOM fractionation—labeled according to compound-class composition resulting from spectral interpretations—is shown in Figure 2. Spectral interpretations of the compound-class composition of tertiary-treated wastewater studied in Los Angeles have been presented previously (*25*). The DOM fractionation and compound-class composition shown in Figure 2 are similar to the DOM fractionation in the Los Angeles study except that the percentage of hydrophilic acid fraction is greater for the 91st Avenue WWTP effluent. Acronyms for the compound classes in Figure 2 refer to (i) sulfonated surfactants composed of linear alkyl sulfonates (LAS) and dialkyltetralin sulfonates (DATS); (ii) sulfonated surfactant metabolites composed of sulfophenyl carboxylates (SPCs), sulfophenyl dicarboxylates (SPDCs), and dialkyltetralin sulfonates dicarboxylates (DATSDCs); and (iii) neutral surfactant metabolites consisting of alkylphenolethoxy carboxylates (APECs) and carboxyalkylphenolethoxy carboxylates (CAPECs). The hydrophobic neutral fraction was colored green, resulting from the use of a mixture of dyes whose major component is the blue dye erioglaucine (*3*). The composition of the 91st Avenue WWTP effluent after passage through the treatment wetland was altered by the input of humic substances. Spectral characterizations and compound-class composition of the wetland effluent are not shown in this paper but generally represent similar structures, as illustrated in Figure 1. Erioglaucine and some aromatic surfactant metabolites fluoresce.

The ^{13}C NMR and FTIR spectra for Salt River (SHPO-A) and Gila River (GHPO-A) hydrophobic acid fractions are shown in Figure 3. The aromatic carbon component (100−160 ppm) of GHPO-A is greater than that of SHPO-A, and SHPO-A contains aromatic sulfonates (FTIR peaks near 1180, 1040, and 1010 cm^{-1}) that are not present in GHPO-A. Hydrophobic acid fractions all contained aromatic carbon, but different aromatic moieties may exhibit different fluorescence spectra.

Fluorescence Emission Spectra of DOM Fractions. Figure 4 presents emission scans (λ_{ex} = 280 nm) for acid, neutral, and base fractions of DOM from the treated wastewater effluent and wetland effluent (see Table 1). The emission scans exhibited nonnormal fluorescence distributions as a function of emission wavelengths, and peak fluorescence intensities occurred at variable locations. Hydrophobic neutral fractions (EHPO-N and EEHPO-N; see Table 1) had the highest fluorescence intensities. The base fractions (E-Base and EE-Base) exhibited slightly lower maximum fluorescence intensities, occurring at longer wavelengths, than the hydrophobic neutral fractions. The hydrophilic acid fractions (EHPI-A and EEHPI-A) had lower maximum fluorescence intensities, occurring at shorter wavelengths, than the hydrophobic acid or base fractions. Emission spectra shapes were similar for DOM entering and exiting the wetland system, except for a secondary fluorescence peak (λ_{em} = 425 nm) that was present in EHPO-N but was less apparent in EEHPO-N.

Fluorescence EEM of DOM Fractions. The broad emission spectra of all the DOM fractions (Figure 4) were attributable to a continuum of organic molecules. EEMs also exhibited fairly broad emission and excitation spectra (Figure 5). DOM fractions had EEM peaks located at different excitation and emission wavelength pairs. For example, SRFA had two EEM peaks associated with longer excitation and emission wavelengths than any DOM fraction of wastewater origin (Figure 5), including comparable fractions based on XAD-8 fractionation (EHPO-A and EEHPO-A). EEMs provide more data than single-emission spectra.

EEM spectra for EBOM, Salt River, and Gila River DOM fractions plus tryptophan (an aromatic amino acid) are presented in Figure 6. EEMs for hydrophobic acids differed depending on the source (GHPO-A, SHPO-A, SRFA, EHPO-A, or EEHPO-A in Figures 5 and 6). The EBOM fraction exhibited EEM features similar to those of tryptophan and EHPI-A. After completion of the study, it was noted that the use of ammonium hydroxide for EBOM extraction could have caused ammonification of the sample. In comparison with previous work by the authors, the EBOM fraction obtained using a sodium hydroxide extraction yielded EEM features similar to those presented in Figure 6 (*31*). Therefore, it was concluded that under the extraction conditions used, extraction with ammonium hydroxide had negligible effects on the EEM.

Quantification of EEM Fluorescence. Using consistent excitation and emission wavelength boundaries for each EEM, horizontal and vertical lines were drawn to divide the EEM into five regions (Figures 5 and 6). We operationally defined excitation and emission boundaries into five regions for this study based largely upon supporting literature (Figure 7). EEM peaks have been associated with humic-like, tyrosine-like, tryptophan-like, or phenol-like organic compounds (*32*−*34*). In general, peaks at shorter excitation wavelengths (<250 nm) and shorter emission wavelengths (<350 nm) are related to simple aromatic proteins such as tyrosine (Regions I and II) (*11*, *35*). Peaks at intermediate excitation wavelengths (250−~280 nm) and shorter emission wavelength (<380 nm) are related to soluble microbial byproduct-like material (Region IV) (*34, 36, 37*). Peaks at longer excitation wavelengths (>280 nm) and longer emission wavelengths (>380 nm) are related to humic acid-like organics (Region V) (*38*−*40*). EEM data for excitation wavelengths shorter than 240 nm have not been widely reported but can be reliably measured with

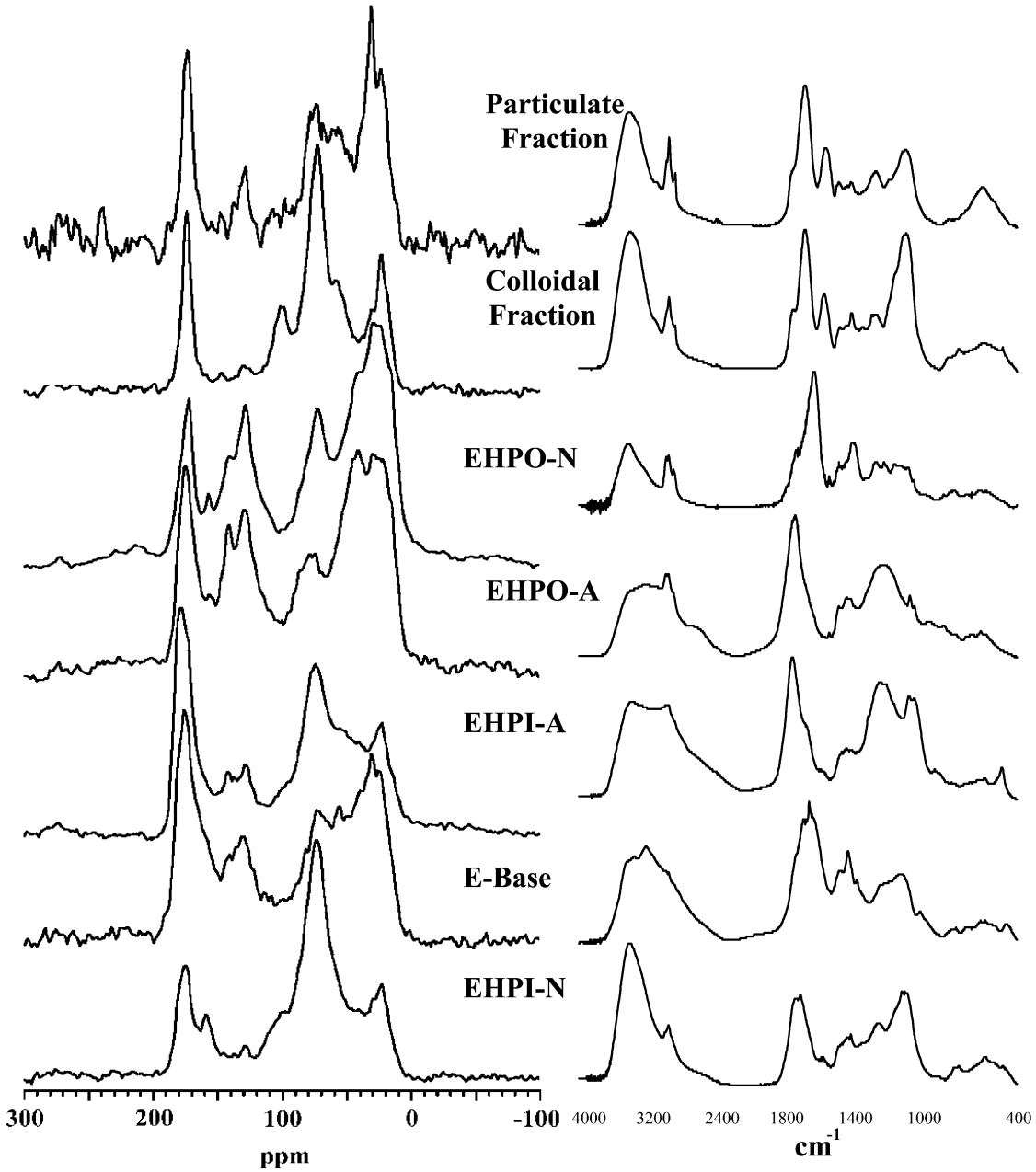

FIGURE 1. ^{13}C NMR (left) and FTIR (right) spectra of DOM fractions (see Table 1) in effluent from the 91st Avenue WWTP (inlet to the pilot wetland system).

fairly recent advances that provide stable source energy at these wavelengths. For fulvic acids, EEMs with minimum excitation wavelengths of 250 nm indicated shoulders of EEM peaks located at shorter excitation wavelengths (*17*). Therefore, peaks at shorter excitation wavelengths (<250 nm) and longer emission wavelengths (>350 nm) are related to fulvic acid-like materials (Region III) (*41*).

The DOM-related literature lacks analytical techniques capable of quantifying multiple broad-shaped EEM peaks. We postulated that integration beneath EEMs within selected regions would represent the cumulative fluorescence response of DOM with similar properties. The FRI technique was developed to integrate the area beneath EEM spectra. The volume (Φ_i) beneath region "*i*" of the EEM can be calculated with

$$\Phi_i = \int_{ex}\int_{em} I(\lambda_{ex}\lambda_{em})\, d\lambda_{ex}\, d\lambda_{em} \quad (1)$$

For discrete data, the volume (Φ_i) was expressed by

$$\Phi_i = \sum_{ex}\sum_{em} I(\lambda_{ex}\lambda_{em})\Delta\lambda_{ex}\Delta\lambda_{em} \quad (2)$$

in which $\Delta\lambda_{ex}$ is the excitation wavelength interval (taken as 5 nm), $\Delta\lambda_{em}$ is the emission wavelength interval (taken as 0.5 nm), and $I(\lambda_{ex},\lambda_{em})$ is the fluorescence intensity at each excitation−emission wavelength pair. Within each of the five FRI regions, 800−10,000 wavelength-dependent fluorescence intensity data points are represented (see *N* in Table 2). The cumulative volume beneath the EEM (Φ_T) was calculated as $\Phi_T = \sum\Phi_i$. All Φ_T and Φ_i values were normalized to a DOC concentration of 1 mg/L for comparison of EEMs from different sources of DOM. The DOC-normalized FRI volume has a unit of AU-nm^2-[mg/L C]$^{-1}$. The percent fluorescence response in a specific region (P_i) was calculated as $\Phi_i/\Phi_T \times 100\%$.

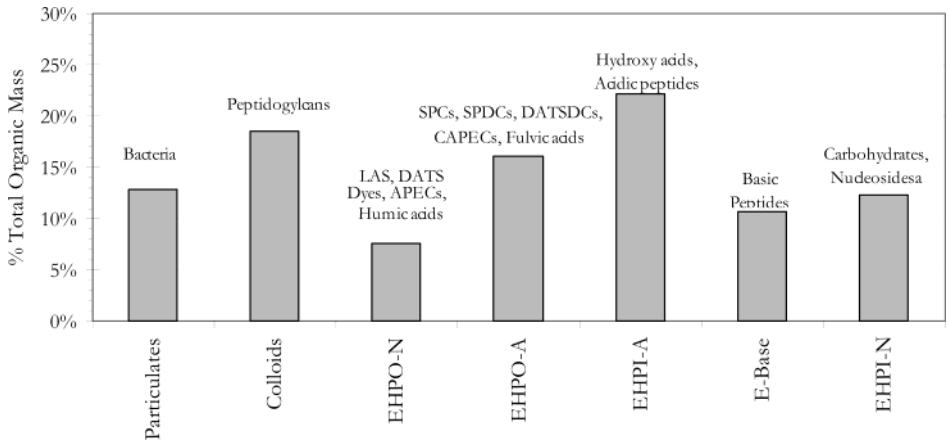

FIGURE 2. Bar diagram of DOM fractions with compound-class composition of effluent from the 91st Avenue WWTP.

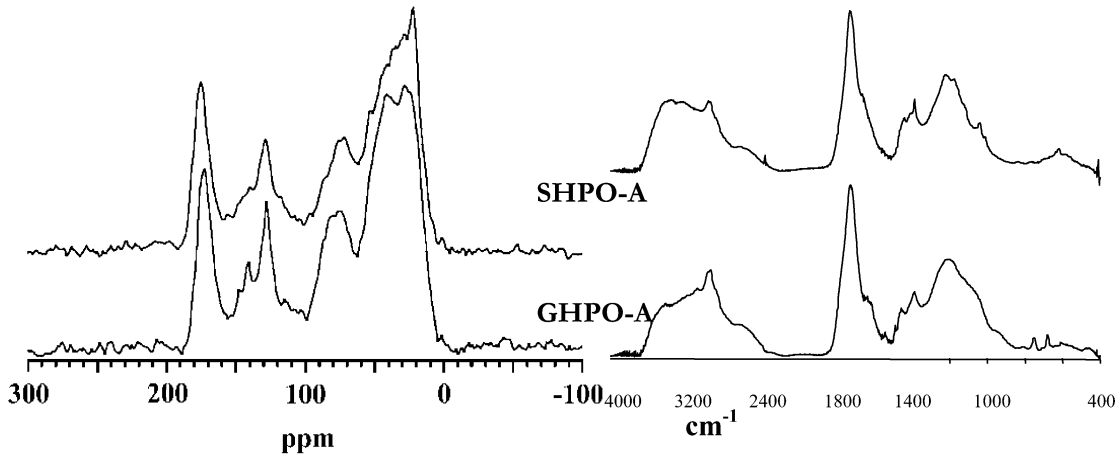

FIGURE 3. ^{13}C NMR (right) and FTIR (left) spectra for the Salt River (SHPO-A) and Gila River (GHPO-A) hydrophobic acid fractions.

TABLE 2. FRI Parameters for Operationally Defined EEM Regions and Volumetric (Φ) and Percentage (P) Values for Triplicate EEM Analysis of SRFA Samples

	FRI parameters				SRFA triplicate analysis				
EEM region	no. of EEM data points per region (N)	projected excitation−emission area (nm^2)	fractional projected area per region	MF$_i$	Φ_i ($\times 10^{-5}$)	P_i (%)	$\Phi_{i,n}$ ($\times 10^{-5}$)	$P_{i,n}$ (%)	CV (%)
I	800	2,000	0.049	20.4	0.17	1	3.5	4	4.0
II	1,000	2,500	0.061	16.4	1.0	5	16	20	0.7
III	3,400	8,500	0.208	4.81	8.4	43	40	49	1.1
IV	5,400	4,664	0.114	8.76	0.65	3	5.7	7	3.1
V	10,200	23,198	0.568	1.76	9.3	48	16	20	0.6
summation	20,800	40,862	1.000		20	100	82	100	

Although inner-filter corrections account for molecular absorbance, they do not account for secondary or tertiary excitation and emission responses or the resultant extension of peaks in the form of shoulders into longer emission scan wavelengths or EEMs. By normalizing Φ_i to relative regional areas (nm^2), we reduced the effects of dominance by shoulders in different EEM regions on overall interpretations. To account for these secondary or tertiary responses at longer wavelengths, a multiplication factor for each region (MF$_i$), equal to the inverse of the fractional projected excitation−emission area, was calculated (Table 2). Normalized excitation−emission area volumes ($\Phi_{i,n}$, $\Phi_{T,n}$) and percent fluorescence response ($P_{i,n}$) were calculated as follows:

$$\Phi_{i,n} = \mathrm{MF}_i \Phi_i \quad (3)$$

$$\Phi_{T,n} = \sum_{i=1}^{5} \Phi_{i,n} \quad (4)$$

$$P_{i,n} = \Phi_{i,n}/\Phi_{T,n} \times 100\% \quad (5)$$

Triplicate EEM analysis of SRFA followed by FRI was used to evaluate the reproducibility of the FRI technique (Table 2). The precise emission wavelength corresponding with the maximum or secondary EEM peak varied by ±5 nm but always was located within consistent EEM regions. Calculated regional EEM volumes had low coefficients of variation (<4%), suggesting that the FRI technique was reproducible. Region I had the highest variability. Normalizing Φ_i by projected regional areas (i.e., $\Phi_{i,n}$) slightly decreased the percentage of EEM volume attributed to Regions III and IV.

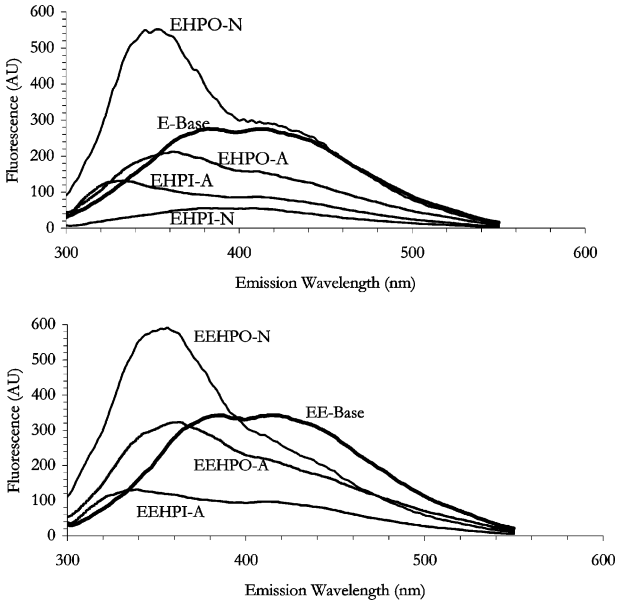

FIGURE 4. Corrected emission fluorescence scans (λ_{ex} = 280 nm) for DOM fractions (see Table 1) from the WWTP effluent (upper) and effluent from the pilot wetland receiving WWTP effluent (lower) (DOC = 1 mg/L; pH 3).

TABLE 3. Percentage Distribution ($f_i \times 100\%$) and Φ_T from FRI Analysis of DOM Fractions

DOM fraction	percentage distribution $\Phi_{T,n}$ $P_{I,n}$ (%)	$P_{II,n}$ (%)	$P_{III,n}$ (%)	$P_{IV,n}$ (%)	$P_{V,n}$ (%)	$\Phi_{T,n}$ ($\times 10^{-6}$) (AU-nm^2-[mg/L C]$^{-1}$)
91st Ave WWTP Effluent						
EHPO-N	25	53	11	9	3	180
E-Base	12	38	30	12	9	64
EHPO-A	28	44	15	8	4	78
EHPI-A	21	45	18	11	5	28
91st Ave WWTP Wetland Effluent						
EEHPO-N	20	51	14	10	4	120
EE-Base	15	33	30	12	10	50
EEHPO-A	28	42	16	9	4	52
EEHPI-N	15	36	26	12	10	8
EEHPI-A	24	42	17	12	5	28
Salt River						
S-Base	12	40	27	12	9	46
SHPO-A	18	47	20	10	5	95
SHPI-A	15	40	26	10	9	23
Gila River						
GHPO-A	5	30	42	9	14	42
Suwannee River						
SRFA	4	20	49	7	20	8
EBOM	18	42	16	17	8	47
tryptophan	14	58	10	17	2	44

Tryptophan and the EBOM fraction had EEM peaks at shorter wavelengths (Figure 6) than SRFA (Figure 5). P_i values for combined Regions III (fulvic-like) and V (humic-like) were 59% and 32% for EBOM and tryptophan, respectively. However, $P_{i,n}$ values for combined Regions III and V were lower (24% and 12%, respectively), as shown in Table 3. Although EBOM may contain humified materials (discussed later), tryptophan does not. Therefore, volumetric interpretations indicate that unintentional amplification of apparent humic- and fulvic-like EEM responses can be avoided by accounting for projected areas (i.e., eqs 3−5). Differences between P_i and $P_{i,n}$ are directly proportional to the operationally defined excitation−emission wavelength boundaries (Figure 7). Shifting the emission boundary between Regions II−V from 390 nm to a longer wavelength would reduce the range in MF_i values, but this shift would also increase Φ_i values for Regions II and IV and decrease Φ_i values for Regions III and V. The net effect of shifting the boundary is minor. Therefore, we believe application of MF_i is appropriate when EEMs spanning wide ranges of excitation and emission wavelengths are compared.

FRI Parameters for Wastewater and Riverine DOM. Figure 8 and Table 3 give $\Phi_{T,n}$ values for 15 DOM fractions from different sources. The continuum of $\Phi_{T,n}$ values illustrates that hydrophobic fractions have quantifiably larger overall fluorescence than base fractions and hydrophilic material. This observation is consistent with ^{13}C NMR data, which generally indicate that hydrophobic fractions have higher aromatic carbon content. Though the volumetric interpretation (i.e., $\Phi_{T,n}$) is consistent with the simple emission scans (Figure 4), the FRI technique is more robust because it encompasses the entire EEM region comprising ~40 emission scans and not just a single emission scan.

The distribution of volumetric fluorescence among the five regions (i.e., $P_{i,n}$) is presented in Table 3. For the wastewater-derived fractions, Salt River fractions, EBOM fraction, and tryptophan, the highest percentage ($38\% < P_{II,n} < 58\%$) of the $\Phi_{T,n}$ occurred in Region II (aromatic proteins). This quantitative result is consistent with visual analysis of the location of EEM peaks within Region II of the delineated regions (Figures 5 and 6). The Salt River fractions tended to have higher $P_{III,n}$ and lower $P_{I,n}$ values than the wastewater-derived samples (Table 3), suggesting that a slightly more humified (humic- or fulvic-like) material was present in the Salt River. In contrast to the other DOM fractions, the highest percentage of the $\Phi_{T,n}$ in GHPO-A and SRFA fractions ($42\% < P_{III,n} < 49\%$) occurred in Region III ($P_{III,n}$; fulvic-like materials). Variability in $P_{i,n}$ values may be used as surrogates for DOM source or dominant structures (discussed in the following paragraph).

The Salt River is a surface water source in which algal- and bacterial-produced DOM may have contributed to the DOC, whereas the wastewater effluent DOM contains bacteria-related soluble microbial products and other refractory materials. The Gila River sample was composed largely of groundwater seepage from agricultural areas. GHPO-A was characterized with a dominant EEM peak in Region III (Table 3). On the basis of hydrologic assessments, the Gila River sample apparently does not contain significant DOM contributions from algae or bacteria. Therefore, the potential differences in DOM sources may be differentiable through the comparison of $P_{i,n}$ values for DOM collected during variable spatial or temporal sampling events.

Fluorescence of Wastewater DOM. Previous work based on DOM fractionation and ^{13}C NMR analysis suggested that treated wastewater effluent contained residual DOM present in drinking water plus soluble microbial products contributed during biological sludge treatment and refractory DOM added by industry, homeowners, and other water users (*42*). The EBOM fraction is assumed to comprise soluble microbial products containing amino acids and carbohydrates (*43*). Because these aromatic amino acids fluoresce, we used tryptophan, an aromatic amino acid, for EEM confirmation of biological activity in natural systems (*32*, *44*). Tryptophan (and tyrosine—not shown) lacked significant FRI in Region V (Figure 6). EBOM was characterized as containing some humic-like material (Region V) and exhibited a distribution of fluorescence response similar to that of tryptophan (Table 3; Figure 6). Both EBOM and tryptophan samples were dominated by fluorescence in Regions II and IV, regions associated with soluble microbial products and other aromatic proteins. Previously it was estimated that ~50% of extracted proteins may be hydrophobic and that 23% was hydrophilic (*45*). EBOM may also contain fluorescing com-

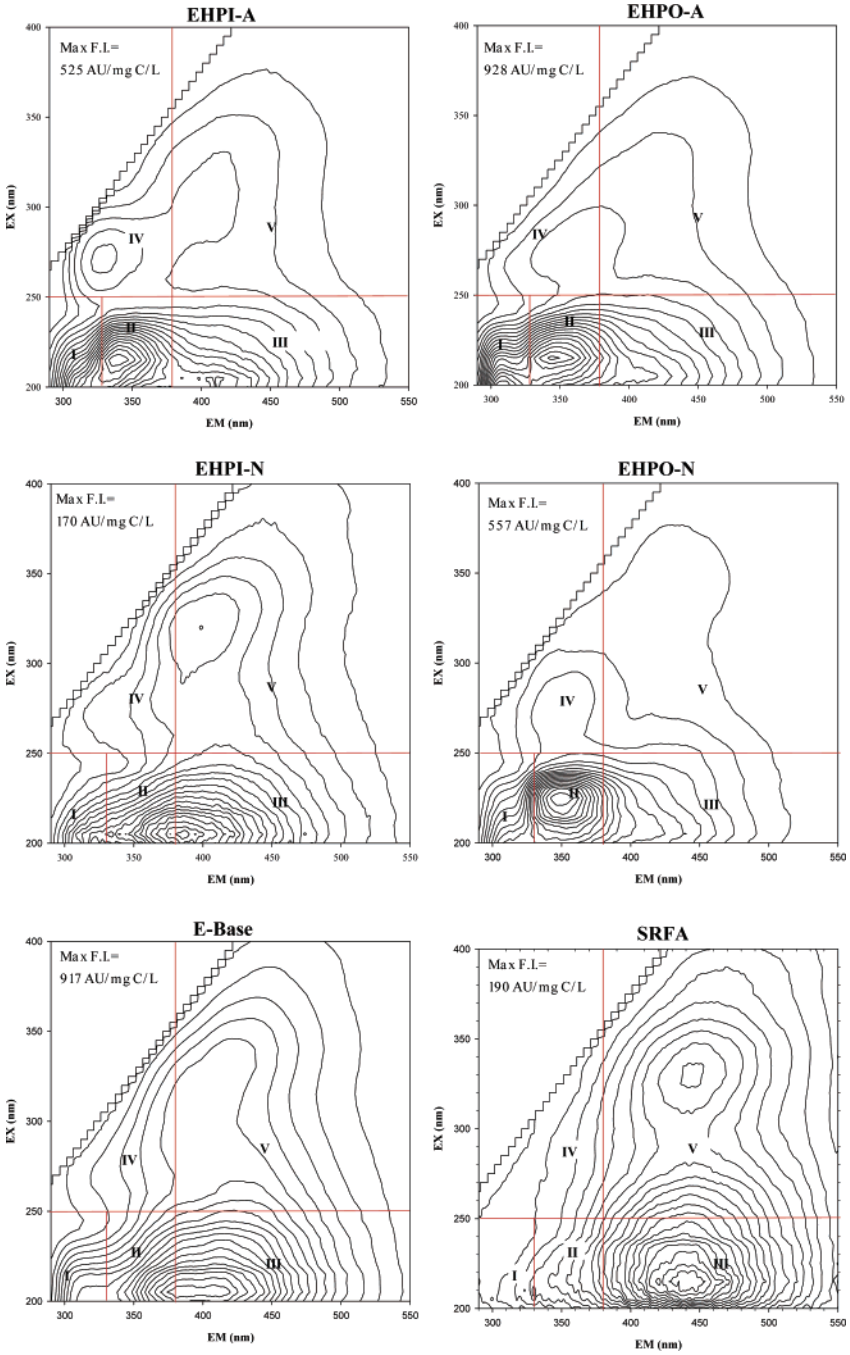

FIGURE 5. EEMs for wastewater effluent DOM fractions and SRFA (see Table 1). Normalized to 1 mg/L C. The maximum fluorescence intensity of each EEM (Max. F.I.) were divided into 20 equal-value contour intervals. Horizontal and vertical lines divide EEMs into five regions (I−V).

pounds or functional groups other than tryptophan. For example, 40−50% of soluble microbial products were observed to be humic, fulvic, and hymathomelanic acids (*46*). EBOM-like material was probably present in the wastewater effluent DOM fractions and thus contributed to the observed EEMs and calculated volumetric values.

Additional samples (nonfractionated) from potable drinking water and treated wastewater sources were examined to characterize the refractory DOM added between drinking water treatment and wastewater treatment. Nonfractionated samples collected from drinking water sources, and hydraulically connected with WWTP effluents had similar EEM characteristics (not shown). These nonfractionated water samples included acid, neutral, and base fractions. Figure 9 presents the $P_{i,n}$ distribution. Drinking water from Mesa (M-DW) came from a surface water source (DOC = 2.5 mg/L) and contained 50% more fulvic-like material ($P_{III,n}$) than drinking water from Tucson (T-DW), which came from groundwater with a low DOC concentration (<0.5 mg/L). In samples collected after wastewater treatment, $P_{I,n}$ and $P_{II,n}$ increased relative to the drinking water samples. This observation is consistent with the production of soluble microbial products (e.g., aromatic proteins) during wastewater treatment. In treated wastewater effluent from Tucson (T-WW) ($\Phi_{T,n} = 2.7 \times 10^7$ AU-nm^2-[mg/L C]$^{-1}$), $\Phi_{T,n}$ was 10 times greater than in the T-DW sample. Likewise, the volumetric fluorescence of treated wastewater effluent from Mesa (M-WW) ($\Phi_{T,n} = 2.3 \times 10^7$ AU-nm^2-[mg/L C]$^{-1}$) was six times greater than that of the M-DW sample. Values for $\Phi_{T,n}$ are DOC-normalized, so the DOM exiting the WWTPs is

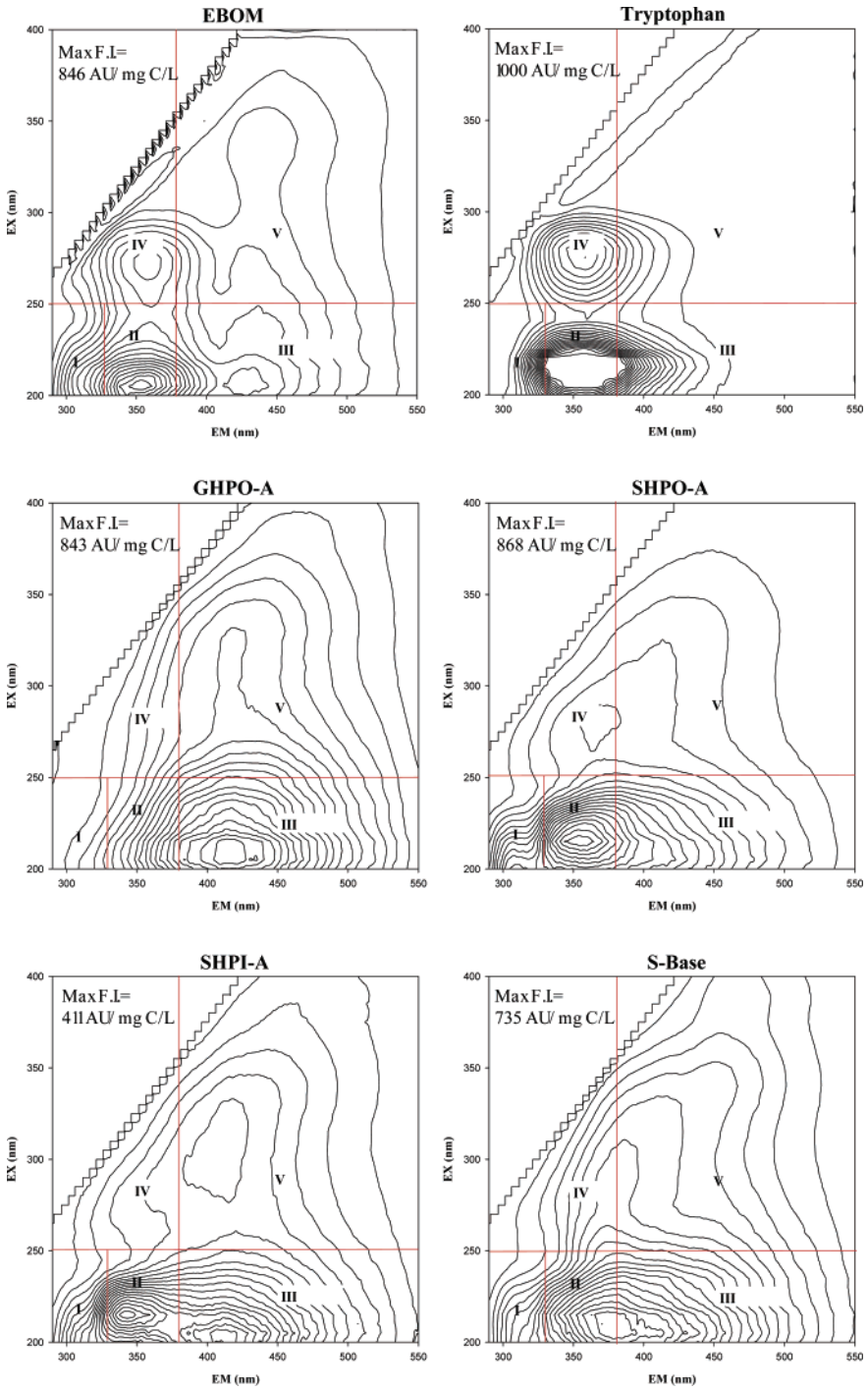

FIGURE 6. EEMs for EBOM, tryptophan, and DOM fractions from the Salt and Gila Rivers (see Table 1). Normalized to 1 mg/L C. The maximum fluorescence intensity of each EEM (Max. F.I.) were divided into 20 equal-value contour intervals. Horizontal and vertical lines divide EEMs into five regions (I−V).

quantitatively more fluorescent than the DOM in drinking water.

These interpretations, along with unpublished data generated with pyrolysis gas chromatography/mass spectrometry and indicating an increase in proteinaceous material between samples from drinking water and samples from WWTP effluent, suggest that soluble microbial products comprise a dominant percentage of the fluorescence in WWTP effluent. WWTP effluents contain aromatic amino acids (e.g., phenylalanine, tyrosine, tryptophan) and aromatic recondensation products (melanoid-like structures) (*45*). WWTP effluents also contain a significant amount of humic and fulvic material. Previous research has shown that much of the humic substances in drinking water is refractory and constitutes part of the DOM in wastewater effluent (*47*). In this study, FRI analysis was able to distinguish a drinking water source from a wastewater source, even a wastewater source containing a strong contribution of DOM from the drinking water.

Comparison of Spectroscopic Properties. Previous work has shown linear correlations between specific ultraviolet absorbance (SUVA—the ratio of the UVA_{254} measurement and the DOC concentration) and aromatic carbon content from liquid-state ^{13}C NMR (*48*, *49*). Similar trends were observed for the DOM fractions characterized in this study. SUVA was correlated with aromatic carbon from solid-state

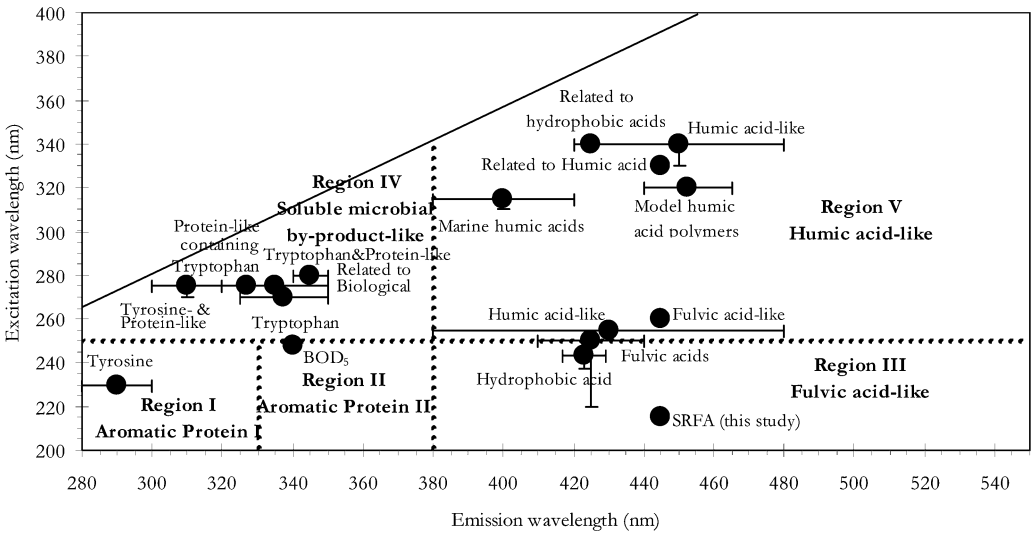

FIGURE 7. Location of EEM peaks (symbols) based on literature reports and operationally defined excitation and emission wavelength boundaries (dashed lines) for five EEM regions.

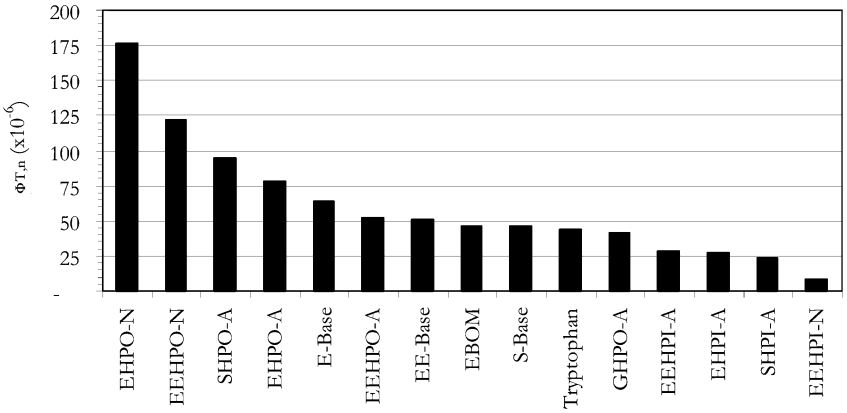

FIGURE 8. Rank order decrease in $\Phi_{T,n}$ (AU-nm^2-[mg/L C]$^{-1}$) for DOM fractions (see Table 1).

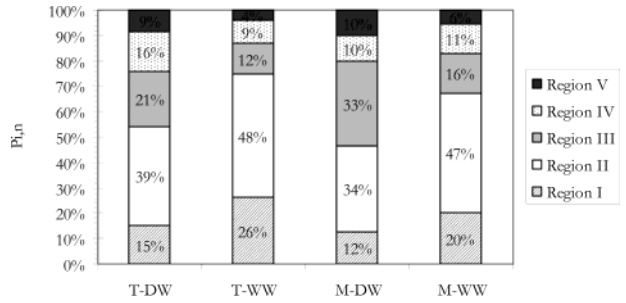

FIGURE 9. Distribution of FRI in nonfractionated DOM from samples of Tucson drinking water (T-DW) and treated wastewater effluent (T-WW) and samples of Mesa drinking water (M-DW) and treated wastewater effluent (M-WW).

^{13}C NMR in the 110−160 ppm range (r^2 = 0.62; N = 7). Correlations between $\Phi_{T,n}$ or most P_i values lacked significant correlation (r^2 < 0.5) with aromatic carbon content, or any other wavelength ranges from solid-state ^{13}C NMR. There was no correlation between $\Phi_{T,n}$ and SUVA. Functional groups or other moieties appear to affect the linear correlation observed between aromatic carbon and fluorescence.

Other researchers have observed linear correlations between the carbon-to-nitrogen ratio and fluorescence intensity at excitation−emission wavelengths that fall within Region IV (*50*). Elemental data on the isolates used in this study were not available. However, DOM fractions characterized by nitrogen-containing moieties from FTIR analysis (broad amide carbonyl peak near 1650 cm^{-1} such as the hydrophilic base fraction in Figure 1) showed higher $\Phi_{T,n}$ values. Fluorescence analysis of model compounds by the authors and others has demonstrated that electron-donating functional groups (e.g., amine, hydroxyl) can significantly increase fluorescence intensities (*51*). With additional research employing the FRI technique the method may be capable of quantifying relative concentrations of π bonds with different electron-donating functional groups or bonded atoms containing electrons (e.g., oxygen, nitrogen, and sulfur).

Applications for the FRI Technique. Regional excitation−emission wavelength boundaries selected to characterize EEMs were operationally defined based on literature reports on dominant EEM peak locations, analysis of DOM fractions, model compounds, and extracted biomass organic matter. These boundaries were developed to characterize surface water and treated wastewater sources from the southwestern United States; use of this approach in other studies may require modification of the regional boundaries. This paper presented an example application of the FRI technique for use in analyzing drinking water and wastewater samples, but many other applications could benefit from the quantitative information provided by FRI. The selected excitation−emission wavelength boundaries should serve as guidance, but the FRI technique could be used with any regional boundaries imposed for specific interests. The FRI technique could be applied to watershed studies of DOM transformation, possibly being able to monitor changes in DOM "composition" along flow paths. This type of analysis would

aid ecologists in studying DOM cycling or sources and engineers in tracking potential wastewater sources in river systems. Changes in $\Phi_{i,n}$ or $P_{i,n}$ may also be helpful in studying metal complexation or organic compound binding, using EEMs in a quantifiable fashion that accounts for the continuum of binding sites.

Acknowledgments

This work was supported by the National Center for Sustainable Water Supply at Arizona State University under the directorship of Dr. Peter Fox. The Bureau of Reclamation provided support for the DOM characterization studies. The authors also thank Dr. Joerg Drewes for providing information on the Mesa and Tucson wastewater treatment plants. This research was part of a research project titled "An Investigation of Soil Aquifer Treatment for Sustainable Water Reuse", which was conducted by a team of faculty and graduate students from Arizona State University, the University of Arizona, the University of Colorado, and Stanford University and was funded by the cities of Phoenix, Mesa, Scottsdale, Tempe, Glendale, and Youngstown, AZ; the Salt River Project; Tucson Water; the USDA Water Conservation Laboratory; the American Water Works Association Research Foundation; the Water Environment Research Foundation; and the National Research Institute. The views and conclusions contained in this paper are those of authors and should not be interpreted as necessarily representing the official policies, either expressed or implied, of the U.S. Geological Survey.

Literature Cited

(1) Manka, J.; Rebhun, M. *Water Res.* **1982**, *16*, 399−403.
(2) Rostad, C. E.; Katz, B. G.; Leenheer, L. A.; Martin, B. S.; Noyes, T. I. *Abstr. Pap. Am. Chem. Soc.* **1999**, *217*, 035-ENVR.
(3) Rostad, C. E.; Martin, B. S.; Barber, L. B.; Leenheer, J. A.; Daniel, S. R. *Environ. Sci. Technol.* **2000**, *34*, 2703−2710.
(4) Korshin, G. V.; Benjamin, M. M.; Sletten, R. S. *Water Res.* **1997**, *31*, 1643−1650.
(5) Leenheer, J. A.; Croue, J. P. *Environ. Sci. Technol.* **2003**, *37*, 18A−26A.
(6) Her, N.; Amy, G.; Foss, D.; Cho, J. W. *Environ. Sci. Technol.* **2002**, *36*, 3393−3399.
(7) Perminova, I. V.; et al. *Environ. Sci. Technol.* **2003**, *37*, 2477−2485.
(8) Leenheer, J. A., et al., Eds. *Comprehensive isolation or organic matter from water for spectral characterization and reactivity testing*; American Chemical Society: Washington, DC, 2000.
(9) U.S. Geological Survey. Humic Substances in the Suwannee River, Georgia: Interactions, properties, and proposed structures. *U.S. Geol. Surv. Water-Supply Pap.* **1994**, *No. 2372*.
(10) Christian, G. D., Callis, J. B., Davidson, E. R., Eds. *Array detectors and excitation−emission matrices in multicomponent analysis*; 1976; Vol. 4.
(11) Ahmad, S. R.; Reynolds, D. M. *Water Res.* **1999**, *33*, 2069−2074.
(12) Cabaniss, S. E.; Shuman, M. S. *Mar. Chem.* **1987**, *21*, 37−50.
(13) Matthews, B. J. H.; Jones, A. C.; Theodorou, N. K.; Tudhope, A. W. *Mar. Chem.* **1996**, *55*, 317−332.
(14) Senesi, N.; Miano, T. M.; Provenzano, M. R.; Brunetti, G. *Sci. Total Environ.* **1989**, *81−2*, 143−156.
(15) Senesi, N.; Miano, T. M.; Provenzano, M. R.; Brunetti, G. *Soil Sci.* **1991**, *152*, 259−271.
(16) Senesi, N., Miano, T. M., Provenzano, M. R., Eds. *Fluorescence spectroscopy as a means of distinguishing fulvic and humic acids from dissolved and sedimentary aquatic sources and terrestrial sources*; Springer-Verlag: New York, 1991.
(17) McKnight, D. M.; et al. *Limnol. Oceanogr.* **2001**, *46*, 38−48.
(18) Battin, T. J. *Org. Geochem.* **1998**, *28*, 561−569.
(19) Donahue, W. F.; Schindler, D. W.; Page, S. J.; Stainton, M. P. *Environ. Sci. Technol.* **1998**, *32*, 2954−2960.
(20) Galapate, R. P.; et al. *Water Res.* **1998**, *32*, 2232−2239.
(21) Marhaba, T. F.; Van, D.; Lippincott, L. *Water Res.* **2000**, *34*, 3543−3550.
(22) Marhaba, T. F.; Pu, Y. *J. Hazard. Mater.* **2000**, *73*, 221−234.
(23) Marhaba, T. F.; Lippincott, R. L. *J. Environ. Eng. ASCE* **2000**, *126*, 1039−1044.
(24) Parlanti, E.; Worz, K.; Geoffroy, L.; Lamotte, M. *Org. Geochem.* **2000**, *31*, 1765−1781.
(25) Leenheer, J. A.; et al. *Environ. Sci. Technol.* **2001**, *35*, 3869−3876.
(26) Seitz, W. R., Ed. Luminescence Spectroscopy, Vol. 1. In *Theory and Practice*, Vol. 7; 1981.
(27) Westerhoff, P.; Chen, W.; Esparza, M. *J. Environ. Qual.* **2001**, *30*, 2037−2046.
(28) Mobed, J. J.; Hemmingsen, S. L.; Autry, J. L.; McGown, L. B. *Environ. Sci. Technol.* **1996**, *30*, 3061−3065.
(29) APHA; WEF. *Standard Methods for the Examination of Water And Wastewater*, 19th ed.; American Public Health Association: Washington, DC, 1998.
(30) Alamany, L. B.; Grant, D. M.; Pubmire, R. J.; Alger, T. D.; Zilm, K. W. *J. Am. Chem. Soc.* **1983**, *105*, 2142−2147.
(31) Esparza-Soto, M.; Westerhoff, P. K. *Water Sci. Technol.* **2001**, *43*, 87−95.
(32) Coble, P. G.; Green, S. A.; Blough, N. V.; Gagosian, R. B. *Nature* **1990**, *348*, 432−435.
(33) Coble, P. G.; Schultz, C. A.; Mopper, K. *Mar. Chem.* **1993**, *41*, 173−178.
(34) Coble, P. G. *Mar. Chem.* **1996**, *51*, 325−346.
(35) Determann, S.; Reuter, R.; Wagner, P.; Willkomm, R. *Deep-Sea Res., Part I* **1994**, *41*, 659−675.
(36) Ismaili, M. M.; Belin, C.; Lamotte, M.; Texier, H. *Oceanol. Acta* **1998**, *21*, 645−654.
(37) Reynolds, D. M.; Ahmad, S. R. *Water Res.* **1997**, *31*, 2012−2018.
(38) Artinger, R.; et al. *Appl. Geochem.* **2000**, *15*, 97−116.
(39) Miano, T.; Sposito, G.; Martin, J. P. *Geoderma* **1990**, *47*, 349−359.
(40) Mounier, S.; Braucher, R.; Benaim, J. Y. *Water Res.* **1999**, *33*, 2363−2373.
(41) Mounier, S.; Patel, N.; Quilici, L.; Benaim, J. Y.; Benamou, C. *Water Res.* **1999**, *33*, 1523−1533.
(42) Drewes, J. E.; Fox, P. *Water Sci. Technol.* **1999**, *40*, 241−248.
(43) Bunch, R. L.; Barth, E. F.; Ettinger, M. B. *J. Water Pollut. Control Fed.* **1961**, *33*, 122−126.
(44) Determann, S.; Lobbes, J. M.; Reuter, R.; Rullkotter, J. *Mar. Chem.* **1998**, *62*, 137−156.
(45) Dignac, M. F.; et al. *Water Res.* **2000**, *34*, 4185−4194.
(46) Rebhun, M.; Manka, J. *Environ. Sci. Technol.* **1971**, *5*, 606−609.
(47) Drewes, J. E.; Jekel, M. *Water Res.* **1998**, *32*, 3125−3133.
(48) Chin, Y. P.; Aiken, G.; Oloughlin, E. *Environ. Sci. Technol.* **1994**, *28*, 1853−1858.
(49) Westerhoff, P.; Aiken, G.; Amy, G.; Debroux, J. *Water Res.* **1999**, *33*, 2265−2276.
(50) Benjamin, M. M.; Croue, J. P.; Reiber, S. *Characterization of natural organic matter in drinking water*; AWWA Research Foundation: Denver, 2000.
(51) Wolfbeeis, O. S., Ed. *The Fluorescence of Organic Natural Products, Part I: Methods and Applications*; Wiley: New York, 1985.

Received for review April 15, 2003. Revised manuscript received September 12, 2003. Accepted September 24, 2003.

ES034354C